A Journal of the Gesellschaft Deutscher Chemiker

Angewandte Chemie

GDCh

International Edition

www.angewandte.org

Accepted Article

Title: Controlling Reaction Selectivity via Surface Termination of Perovskite Catalysts

Authors: Felipe Polo-Garzon, Shi-Ze Yang, Victor Fung, Guo Shiou Foo, Elizabeth Erin Bickel, Matthew F. Chisholm, De-en Jiang, and Zili Wu

To be cited as: *Angew. Chem. Int. Ed.* 10.1002/anie.201704656
Angew. Chem. 10.1002/ange.201704656

Link to VoR: http://dx.doi.org/10.1002/anie.201704656
http://dx.doi.org/10.1002/ange.201704656

WILEY-VCH

10.1002/anie.201704656

WILEY-VCH

Controlling Reaction Selectivity via Surface Termination of Perovskite Catalysts

Felipe Polo-Garzon[1], Shi-Ze Yang[2], Victor Fung[3], Guo Shiou Foo[1], Elizabeth E. Bickel[4], Matthew F. Chisholm[2], De-en Jiang[3], Zili Wu*[1]

Abstract: *Although perovskites have been widely used in catalysis, tuning their surface terminations to control reaction selectivities has not been well established. In this work, we employ multiple surface sensitive techniques to characterize the surface termination (one aspect of surface reconstruction) of $SrTiO_3$ (STO) after thermal pretreatment (Sr-enrichment) and chemical etching (Ti-enrichment). We show, using the conversion of 2-propanol as a probe reaction, that the surface termination of STO can be controlled to greatly tune catalytic acid/base properties and consequently the reaction selectivities in a wide range, which are inaccessible using single metal oxides, either SrO or TiO_2. Density functional theory (DFT) calculations well explain the selectivity tuning and reaction mechanism on different surface terminations of STO. Similar catalytic tunability is also observed on $BaZrO_3$, highlighting the generality of the finding from this work.*

Perovskites are metal oxides with the general formula ABO_3, where A represents a lanthanide, alkali or alkaline earth metal and B represents a transition metal. The cations A and B can have a variety of oxidation states ($A^{+2}B^{+4}O_3$, $A^{+3}B^{+3}O_3$, and $A^{+1}B^{+5}O_3$). Also, the oxidation states can differ from the ideal structure, ABO_3, when the perovskite is oxygen deficient or rich [1]. These materials have shown high oxygen mobility, high tolerance for metal substitutions into the lattice structure, excellent thermal stability (up to 1000 °C) and resistance to sintering of substituted metals. These attributes have driven interest toward perovskite materials, in particular for redox catalysis (e.g. methane reforming, CO oxidation, NO oxidation), whereas acid-base catalysis is yet to be extensively studied[1-2]. In the past five decades, researchers have unsuccessfully attempted to relate catalytic properties of bulk mixed oxides to bulk properties of the crystal structure, such as the short metal-oxygen bond. This is due to the fact that the catalytic "stage", i.e., the surface of a complex oxide can be different from the bulk in both composition and structure, which has highlighted the need for surface sensitive characterization of these materials to comprehend their catalytic behavior.[3] This is also true for perovskites where surface reconstruction has been extensively observed in surface science studies of single crystal or thin film forms. $SrTiO_3$ (STO) is among the most studied perovskites due to its applications in catalysis[4], its extensive use for the growth of important thin films, and its use as an insulating layer for potential field effect device applications and fundamental research[5].

The surface reconstruction of STO is found to be quite complex, depending on treatment temperature, environment and time. Also, these reconstructions have shown to be reversible under certain conditions[6]. Druce et al.[7] and Ngai et al.[8] found A-cation enrichment at the surface after annealing perovskites in oxygen at 1000 °C for 12 h and at 1300 °C for 30 min, respectively. Dagdeviren et al.[6] and Nishimura et al. [9] reported Sr migration to the surface in STO and oxygen depletion during UHV annealing. Contradictorily, Jiang and Zegenhagen[10] concluded that the SrO layer is less stable at high temperature (950 – 1100 °C) both in UHV and in oxygen. Erdman et al. studied the reconstruction of $SrTiO_3$ (001) and reported single Ti-rich overlayer arranged as TiO_{6-x} polyhedra, in contrast to TiO_6 polyhedra in the bulk, after annealing under oxygen up to 1000 °C.[11] However, *ab initio* computational work by Heifets et al.[12] does not support the (2×1) double-layer (DL) TiO_2-terminated surfaces observed by Erdman et al.[11b] This discrepancy reflects the complex dependence of surface structure on treatment conditions; furthermore, observed terminations could be due to kinetic processes far from thermodynamic equilibrium. Additionally, recent work[13] reported the thin-film-like structure of octahedral titania that the surface of STO can adopt, highlighting the complexity of STO surface reconstruction.

In addition to thermal treatment, chemical treatment under an acidic environment has been reported.[9, 14] It has also been reported that Sr-O, Ti-O and mixed terminations of STO nanoparticles depend upon the synthesis procedure;[15] however, their stability under reaction conditions for heterogeneous catalysis was not reported.

Studies on the interaction of select adsorbates (H_2O, NO, CO, CO_2, H_2, O)[16] with specific terminations of STO and other perovskites have been examined. However, to the best of our knowledge, a comprehensive study on tuning reaction selectivity via controlling the surface termination of perovskite catalysts is not present and is reported for the first time in this work.

The present work successfully couples the observed surface terminations via top-surface sensitive characterization techniques with *ab initio* simulation and catalytic performance of STO for dehydrogenation/dehydration (acetone/propene production, respectively) of 2-propanol. Thermal and chemical pretreatments were performed on the samples while conserving their crystal structure as shown via X-ray Diffraction (XRD) (see Supporting Information, Figure S1).

Commercially obtained STO was thermally pretreated in-situ in a plug-flow reactor at 550 °C under 50 mL/min 5%O_2/He for different time periods. After each pretreatment, the conversion of 2-propanol at 303 °C was carried out in a plug-flow reactor (conversion ≤ 13%). As observed in *Figure 1a*, longer pretreatment times greatly increased the rate of acetone production (dehydrogenation) from 0.15 to ~0.60 μmol/m^2/min, decreased the rate of propene production (dehydration) from ~0.32 to ~0.19 μmol/m^2/min; and therefore, decreased the selectivity toward propene. The possible role of different amounts of residual carbonates on STO after different pretreatment durations is excluded as co-feeding CO_2 with 2-propanol does not change the catalytic performance of STO pretreated for 5 hours (see Figure S2a). It is thus hypothesized that longer pretreatment times favor the exposure of Sr-atoms,

[1] F. Polo-Garzon, G. S. Foo, Z. Wu
Chemical Sciences Division and Center for Nanophase Materials Sciences, Oak Ridge National Laboratory
Oak Ridge, Tennessee 37831, United States
E-mail: wuz1@ornl.gov
[2] S. Yang, M. F. Chisholm
Materials Science and Technology Division, Oak Ridge National Laboratory
Oak Ridge, Tennessee 37831, United States
[3] V. Fung, D. Jiang
Department of Chemistry, University of California
Riverside, California 92521, United States
[4] E.E. Bickel
Department of Chemical Engineering, Tennessee Technological University
Cookeville, Tennessee 38505, United States

10.1002/anie.201704656

since basic sites (predominant on a SrO surface termination as shown in Figure S3a-b) favor the dehydrogenation product, acetone[17].

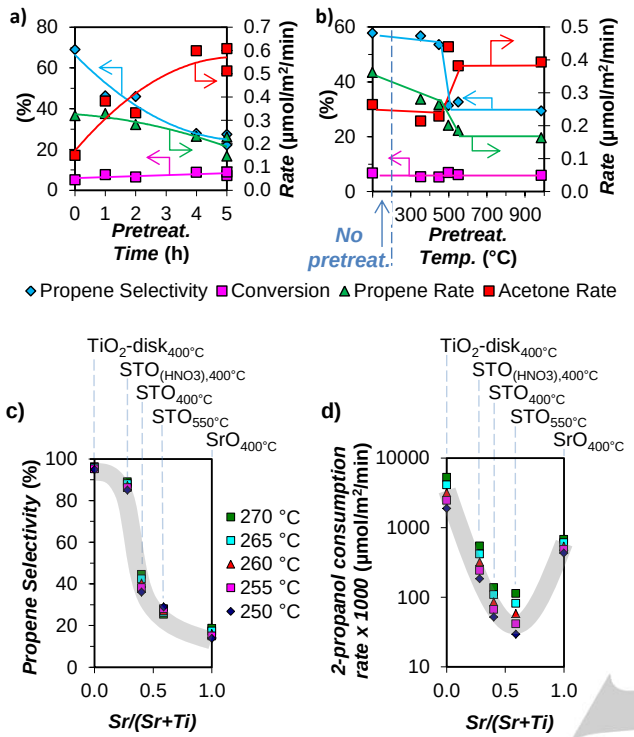

Figure 1 Steady-state conversion of 2-propanol **(a)** at 303 ± 1 °C over STO after different pretreatment times at 550 °C under 50 mL/min 5%O_2/He, and, **(b)** at 300 ± 1 °C after different pretreatment temperatures under 50 mL/min 5%O_2/He for 5 h (1h at 985 °C). **(c)** Propene selectivity, and **(d)** 2-propanol consumption rate (log scale) for conversion of 2-propanol at 250-270 °C over $STO_{400°C}$, $STO_{550°C}$, $STO_{(HNO3),400°C}$, TiO_2-$disk_{400°C}$ and $SrO_{400°C}$ catalysts. Reaction conditions: 50 mL/min Ar, 30 mg of catalyst, WHSV = 0.8 h^{-1}. The subscript next to catalyst name indicates the pretreatment temperature under 50 ccm 5%O_2/He for 5 h before kinetic data were collected.

To test this hypothesis, low energy ion scattering (LEIS) characterization was performed to determine the composition of the top atomic monolayer of material (~0.3 nm)[18] before and after thermal pretreatment. At the surface, STO presented a Sr-to-Ti ratio around 0.7 before thermal pretreatment and 1.4 after thermal pretreatment at 500 °C in O_2 for 30 min (see *Figure 2a*), confirming the exposure of more Sr atoms upon thermal treatment at 500 °C under oxygen. In addition, it is observed that after 4 to 5 hours of thermal treatment, the catalytic performance of STO does not change considerably. These results are in good agreement with the results reported by Bachelet et al.[19], where the SrO termination of STO substrates can be varied from 0% to 100% when annealing at 1300 °C under air for different periods of time (2 – 72 h).

Conversion of 2-propanol was also evaluated on STO after in-situ pretreatment at different temperatures for 5 h under 50 mL/min of 5%O_2/He. After each pretreatment, the conversion of 2-propanol at 300 °C was carried out and the results are shown in *Figure 1b*. For pretreatment temperatures between 450 and 500 °C, the selectivity toward propene decreases significantly from 54% at 450 °C to 31% at 500 °C. However, for pretreatment temperatures above 500 °C the catalytic performance does not change. Thus, it is hypothesized that an increase in the pretreatment temperature exposes more Sr atoms at the surface but reaches a maximum for pretreatment temperatures above ~500 °C. When the thermally pretreated catalyst is held at room temperature for an extended period of time (at least for more than 2 weeks), the effect of the thermal pretreatment is reversed, i.e., propene dominates over acetone for 2-propanol reaction over such a sample. It appears Sr-exposure decreases upon storage of STO at room temperature. This is confirmed by the LEIS analysis as shown in Figure 2a, where the Sr-to-Ti ratio increases after treatment at 500°C. However, this reverse process is not due to exposure to CO_2 or H_2O in the air, as confirmed experimentally (see Figure S2). The kinetics of the reverse process at room temperature, once the thermal pretreatment is performed, are interesting and warrant further investigation.

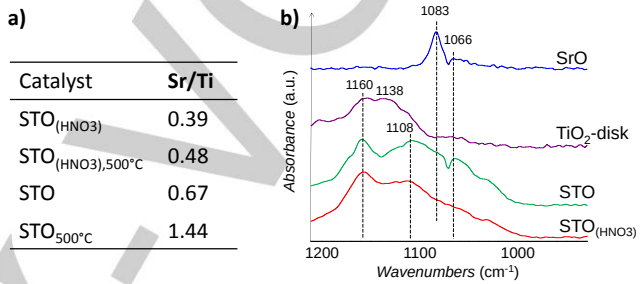

Figure 2 **(a)** Top surface Sr/Ti cation intensity ratio of the pretreated STO and $STO_{(HNO3)}$ catalysts measured using LEIS. The subscript next to catalyst name indicates the temperature at which the materials were pretreated in-situ before LEIS analysis. **(b)** FTIR spectra of methanol adsorption on SrO, TiO_2-disk, STO and $STO_{(HNO3)}$ catalysts at 25 °C. All samples were pretreated at 550 °C under oxygen.

To promote the exposure of the Ti-terminated surface, ex-situ pretreatment in 0.2 M HNO_3 was performed on STO ($STO_{(HNO3)}$) to remove the outmost SrO layer, as performed by Peng et al.[14a] on $La_{0.5}Sr_{0.5}CoO_3$. X-ray photoelectron spectroscopy (XPS) performed on such $STO_{(HNO3)}$ showed no remaining nitrogen (see Figure S4). Additionally, LEIS characterization (Figure 2a and Figure S5-S6) confirmed further exposure of Ti-atoms after treatment with HNO_3 (Sr/Ti = 0.4), and it was found that thermal pretreatment of the washed sample, $STO_{(HNO3),500°C}$, achieved minor exposure of the Sr atoms (Sr/Ti = 0.5), far from the Sr-exposure of the non-washed thermally treated sample, $STO_{500°C}$ (Sr/Ti = 1.4).

High-angle annular dark-field (HAADF) scanning transmission electron microscopy (STEM) was performed on these differently treated STO samples to directly visualize the atomic structure of the surfaces. $STO_{(HNO3)}$ was imaged after in-situ heating at 400°C under vacuum and after ex-situ thermal pretreatment under N_2 at 550°C for 5 h. STO was imaged before and after ex-situ thermal pretreatment under N_2 at 550°C for 5 h (see *Figure 3*). It is clearly observed that the surface of $STO_{(HNO3)}$ is predominantly enriched with single and double layers of Ti. Also, heat treatment at 550 °C did not significantly affect the surface segregation of Ti for the chemically etched sample, which is in good agreement with LEIS results. The STO sample without heat treatment shows similar surface composition dominated with Ti but with minor presence of Sr. However, surface enrichment with Sr is clearly observed when heat treatment at 550 °C is performed. For all STO samples, the (100) plane is confirmed as the main plane exposed at the surface with minor (110) truncation at the corners (see complete set of images in Figure S7); therefore, our DFT calculations are performed upon this major plane.

10.1002/anie.201704656

To study the relation between the exposure of Sr/Ti atoms and the selectivity toward dehydrogenation/dehydration, SrO (obtained commercially) and anatase TiO_2-disk (terminated by large percentage with the (100) plane)[20] were compared with pretreated STO samples. To compare the types of sites encountered in the strontium titanate samples with the sites in SrO and TiO_2-disk, methanol adsorption followed by FTIR spectroscopy was performed (*Figure 2b*). Vibrational spectra of adsorbed methanol on both $STO_{550°C}$ and $STO_{(HNO3),550°C}$ samples reveal spectral features resembling those present on both SrO and TiO_2-disk, with $STO_{(HNO3),550°C}$ closer to TiO_2-disk and $STO_{550°C}$ closer to SrO, further supporting the surface enrichment as analyzed by LEIS and STEM. The observation of different methanol species on both STO samples suggests a synergistic effect rising from the coexistence of Sr and Ti at the surface (details in Supporting Information, section S 2.7). To quantify the concentration and strength of basic and acid sites, adsorption microcalorimetry measurements were performed with CO_2 and NH_3, respectively. In general, the result (Figure S3a-b) showed that $STO_{550°C}$ has more basic sites but fewer acidic sites when compared with $STO_{(HNO3),550°C}$, which is consistent with the higher Sr/Ti ratio on the former STO sample. Nonetheless, the strength (Figure S3a-b) of the basic or acid sites approaching zero surface coverage does not directly correlate with the density of the sites (μmol/m^2) (Table S3) or with the fraction of Sr at the outermost layer [Sr/(Sr+Ti)] (Table S3). This synergistic effect can be explained due to the presence of Sr-O or Ti-O sublayers that together tune the basic/acid properties of the surface (see further details in Supporting Information, section S 2.3).

The heat of adsorption of 2-propanol was also measured. Noticeably, the adsorption strength of 2-propanol does not vary significantly amongst three of the samples studied (STO, $STO_{(HNO3)}$, and TiO_2-disk), suggesting that the adsorption strength of 2-propanol is similar on Ti and Sr sites, except when more than one SrO layer is stacked at the surface, which is the case of the pure SrO catalyst (where CO_2 adsorption may involve reaction to form $SrCO_3$). DFT calculations revealed dissociate adsorption of 2-propanol on the Sr-terminated surface and chemisorption that easily leads to dissociation on the Ti-terminated surface. On the Ti-terminated surface, the reaction energy (ΔH_{rxn}) for dissociation of 2-propanol and the corresponding activation barrier (ΔE_{act}) are -0.33 and 0.18 eV, respectively. The calculated adsorption energies for dissociated 2-propanol on Sr and Ti-terminated surfaces of STO were 135 and 112 kJ/mol, respectively (see Figure S8 – S12), setting the boundary for the strongest adsorption energy (at coverage approaching zero) of 2-propanol on the STO catalyst where both Sr and Ti-terminated surfaces are present. This range (between 135 and 112 kJ/mol) is in good agreement with the experimental values ranging from 110 to 103 kJ/mol (Figure S3c).

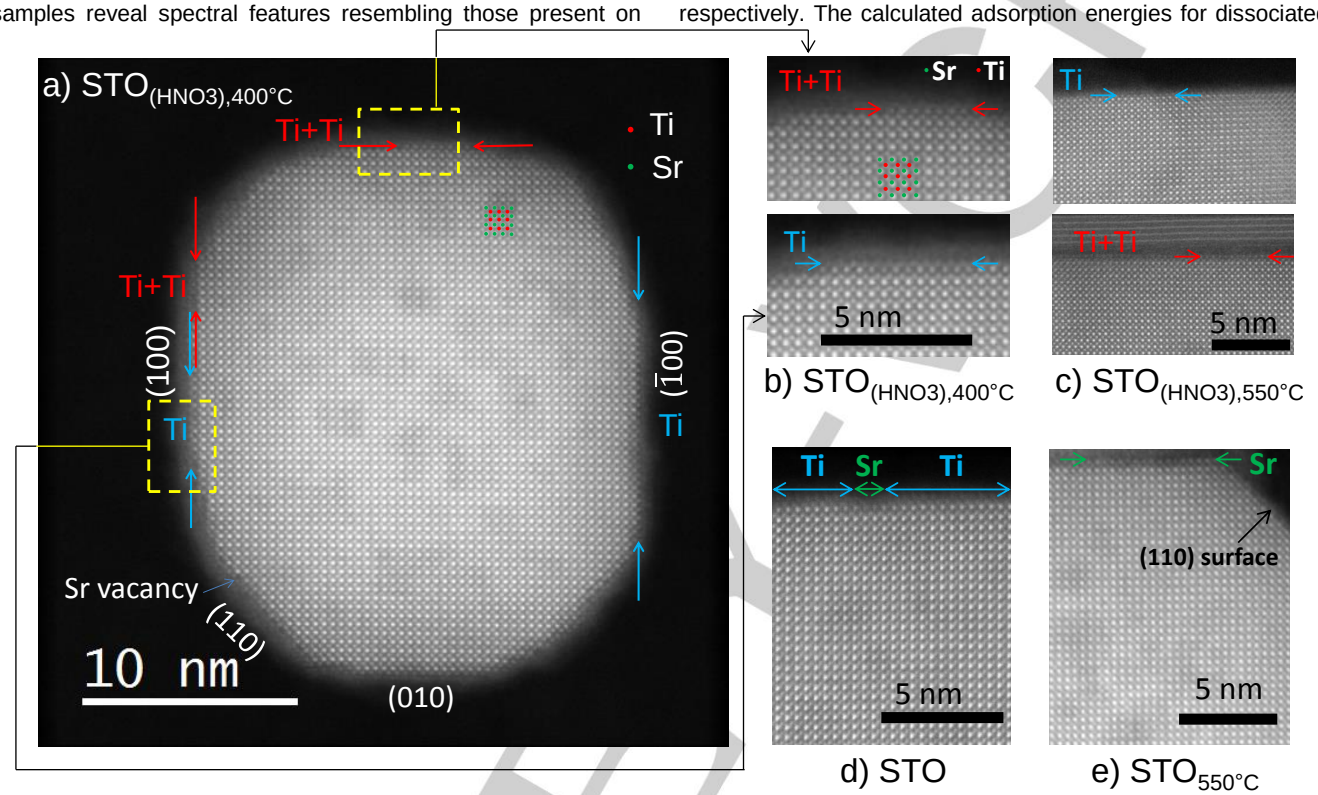

Figure 3 HAADF STEM images of $STO_{(HNO3)}$ after heat treatment at **(a)(b)**400°C and **(c)** 550°C; as well as images of STO **(d)** before and **(e)** after heat treatment at 550°C.

To further understand our experimental observation of the selectivity changes upon different conditioning of STO, DFT was employed to probe the reaction pathways of 2-propanol on the Ti- and Sr-terminated STO (100) surfaces. These surfaces are a simplified version of the more complicated real surfaces; therefore, they are used to shed light on reactivity trends and comparisons to experimental results are rather qualitative. The results (see section S 2.8 in Supporting Information) suggest that both dehydrogenation and dehydration of 2-propanol involve initial deprotonation to generate the 2-propanoxy intermediate; then, depending upon the basicity of the adjacent surface oxygen, either the C_β-H or C_α-H bond is cleaved to produce propene or acetone, respectively. This reaction mechanism is denoted as the E_{1cB} pathway and it is expected from the weak acidity of the surface sites in STO[21]. As shown in *Figure 4*, the rate-determining step (RDS) for acetone formation is the cleavage of the C_α-H bond and for propene formation is the

concerted breaking of the C_β-H and C-O bonds. Calculations show that the Ti-terminated surface of STO favors the production of propene ($\Delta E_{a,propene}$ = 145 kJ/mol, $\Delta E_{a,acetone}$ = 155 kJ/mol) and the Sr-terminated surface favors the production of acetone ($\Delta E_{a,propene}$ = 235 kJ/mol, $\Delta E_{a,acetone}$ = 149 kJ/mol), which agrees well with our experimental observations.

Apparent activation energies were calculated by fitting the Arrhenius equation to kinetic data (Figure S13, Table S4) collected at differential conditions (conversion ≤ 13%)[21] and used to compare reactivity data at the same temperature for the five samples: TiO_2-disk$_{400°C}$, $SrO_{400°C}$, $STO_{(HNO3),400°C}$, $STO_{400°C}$ and $STO_{550°C}$. Apparent activation energies for acetone production on surface-Sr-rich STO ($STO_{550°C}$) (163 kJ/mol) and for propene production on a surface-Ti-rich STO ($STO_{(HNO3),400°C}$) (130 kJ/mol) showed general agreement with the magnitude of the DFT-calculated activation energies for the RDS; namely, 149 and 145 kJ/mol, respectively. Here we note that although the good agreement between our DFT barriers of the rate-limiting steps and the experimental apparent activation energies does shed light on the reaction mechanisms on the two different terminations, a proper reaction kinetic analysis is warranted in the future to firmly establish a relationship between the DFT-predicted mechanism and the experimental kinetic data.

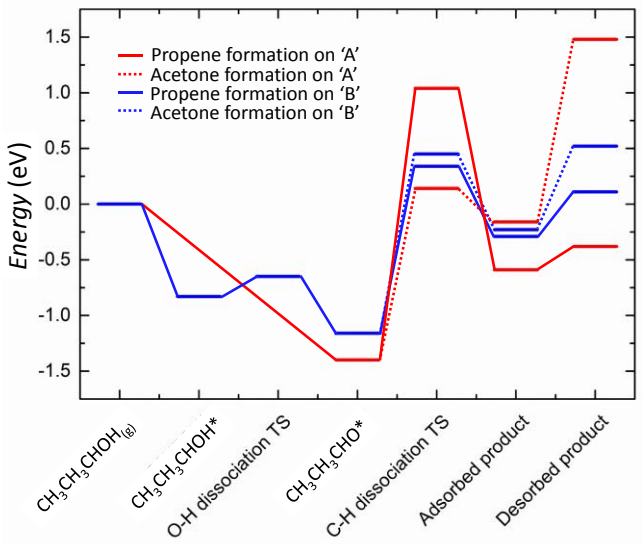

Figure 4 Minimum-energy paths for conversion of 2-propanol over Sr-terminated (A) and Ti-terminated (B) surfaces of STO(100) to propene and acetone.

The unique tunability of reaction selectivity from induced surface terminations of STO is evident from the comparison with the individual single oxides. As seen in *Figure 1*c, in the range 250-270 °C, TiO_2-disk$_{400C}$ and $SrO_{400°C}$ have around 95% and 15% selectivity towards propene, respectively. The perovskite samples enabled to access propene selectivities ranging from 25 to 87 % by tuning their surface composition. *Figure 1d* suggests that the coexistence of Sr and Ti atoms at the surface with composition around 28 – 59 % Sr induces lower rates for both dehydrogenation and dehydration. Since deprotonation of 2-propoxy is assisted by the nearby surface oxygen; for a mixed Sr-Ti surface, with different basicities, protonation/deprotonation processes may simultaneously occur, which reflects on a reduction on 2-propanol consumption rate for STO catalysts. Also, adsorption microcalorimetry measurements suggest that sub-surface layers may tune the acidity and basicity of the surface (see details in Supporting Information, section S 2.3), which can potentially interfere with the rate of protonation/deprotonation. Despite the decrease in reaction rate, perovskite catalysts allow to control the ratio of dehydrogenation and dehydration rates due to the synergy between acid and base sites as observed through FTIR spectroscopy and adsorption microcalorimetry experiments.

In conclusion, we show, using the conversion of 2-propanol as a probe reaction, that altering the surface termination of $SrTiO_3$ allows tuning its acid/base catalytic properties, providing selectivities inaccessible using single metal oxides, namely, SrO and TiO_2. Controlled enrichment of Sr or Ti at the surface of $SrTiO_3$, attained via thermal and chemical treatments was revealed via LEIS and HAADF-STEM. Methanol adsorption followed by FTIR spectroscopy along with adsorption microcalorimetry measurements revealed the synergistic nature of the surface Sr and Ti sites for 2-propanol conversion. DFT calculations were in good agreement with experimental data and showed that both the dehydrogenation and dehydration pathways proceed via the 2-propoxy intermediate. Furthermore, the work expanded to $BaZrO_3$ (Figure S15) suggests that the potential of utilizing the induced surface termination of perovskites for controlling catalytic selectivity is general. The finding of this work has significant implication for catalysis by mixed oxides where the surface and bulk compositions can be different depending on treatment and reaction conditions. Advantages are yet to be taken of the surface terminations of these materials as a unique route to tune the catalytic performances. It also underscores the importance and necessity of surface sensitive characterization of bulk mixed oxides (prior to and post reaction, ideally under reaction conditions) for unambiguous structure – catalysis correlations.

Experimental Section

See Supporting Information, *S 1. Experimental Procedures*.

Acknowledgements

This research is sponsored by the U.S. Department of Energy, Office of Science, Office of Basic Energy Sciences, Chemical Sciences, Geosciences, and Biosciences Division. Part of the work including FTIR, BET and kinetic measurement was conducted at the Center for Nanophase Materials Sciences, which is a DOE Office of Science User Facility. This research used resources of the National Energy Research Scientific Computing Center, a DOE Office of Science User Facility supported by the Office of Science of the U.S. Department of Energy under Contract No. DE-AC02-05CH11231. Electron microscopy at Oak Ridge National Laboratory (S.Z.Y. and M. F. C.) was supported by the U.S. Department of Energy, Office of Science, Basic Energy Sciences, Materials Science and Engineering Division. The authors thank Henry Luftman (Lehigh University) for performing the LEIS analysis and Zach Hood (graduate student at Georgia Institute of Technology) for performing XPS measurements.

Keywords: surface termination, perovskite, acid/base catalysis, selectivity, dehydration/dehydrogenation.

[1] a) S. Royer, D. Duprez, F. Can, X. Courtois, C. Batiot-Dupeyrat, S. Laassiri, H. Alamdari, *Chemical Reviews* **2014**, *114*, 10292-10368; b) H. Zhu, P. Zhang, S. Dai, *ACS Catal.* **2015**, *5*, 6370-6385.
[2] D. Pakhare, J. Spivey, *Chemical Society Reviews* **2014**, *43*, 7813-7837.
[3] a) I. E. Wachs, K. Routray, *ACS Catalysis* **2012**, *2*, 1235-1246; b) S. V. Merzlikin, N. N. Tolkachev, L. E. Briand, T. Strunskus, C. Wöll, I. E. Wachs, W. Grünert, *Angew. Chem. Int. Ed.* **2010**, *49*, 8037-8041.
[4] a) J. M. P. Martirez, S. Kim, E. H. Morales, B. T. Diroll, M. Cargnello, T. R. Gordon, C. B. Murray, D. A. Bonnell, A. M. Rappe,

J. Am. Chem. Soc. **2015**, *137*, 2939-2947; b) J. G. Mavroides, J. A. Kafalas, D. F. Kolesar, *Appl. Phys. Lett.* **1976**, *28*, 241-243; c) R. Konta, T. Ishii, H. Kato, A. Kudo, *J. Phys. Chem. B* **2004**, *108*, 8992-8995; d) K. Iwashina, A. Kudo, *J. Am. Chem. Soc.* **2011**, *133*, 13272-13275; e) J. W. Liu, G. Chen, Z. H. Li, Z. G. Zhang, *J. Solid State Chem.* **2006**, *179*, 3704-3708.

[5] a) C. Aruta, J. Zegenhagen, B. Cowie, G. Balestrino, G. Pasquini, P. G. Medaglia, F. Ricci, D. Luebbert, T. Baumbach, E. Riedo, L. Ortega, R. Kremer, J. Albrecht, *Phys. Status Solidi A* **2001**, *183*, 353-364; b) R. Droopad, Z. Yu, J. Ramdani, L. Hilt, J. Curless, C. Overgaard, J. L. Edwards Jr, J. Finder, K. Eisenbeiser, W. Ooms, *Mater. Sci. Eng. B* **2001**, *87*, 292-296; c) X. X. Xi, Q. Li, C. Doughty, C. Kwon, S. Bhattacharya, A. T. Findikoglu, T. Venkatesan, *Appl. Phys. Lett.* **1991**, *59*, 3470-3472.

[6] O. E. Dagdeviren, G. H. Simon, K. Zou, F. J. Walker, C. Ahn, E. I. Altman, U. D. Schwarz, *Phys. Rev. B* **2016**, *93*, 195303.

[7] J. Druce, H. Tellez, M. Burriel, M. D. Sharp, L. J. Fawcett, S. N. Cook, D. S. McPhail, T. Ishihara, H. H. Brongersma, J. A. Kilner, *Energy Environ. Sci.* **2014**, *7*, 3593-3599.

[8] J. H. Ngai, T. C. Schwendemann, A. E. Walker, Y. Segal, F. J. Walker, E. I. Altman, C. H. Ahn, *Advanced Materials* **2010**, *22*, 2945-2948.

[9] T. Nishimura, A. Ikeda, H. Namba, T. Morishita, Y. Kido, *Surf. Sci.* **1999**, *421*, 273-278.

[10] Q. D. Jiang, J. Zegenhagen, *Surf. Sci.* **1999**, *425*, 343-354.

[11] a) N. Erdman, O. Warschkow, M. Asta, K. R. Poeppelmeier, D. E. Ellis, L. D. Marks, *J. Am. Chem. Soc.* **2003**, *125*, 10050-10056; b) N. Erdman, K. R. Poeppelmeier, M. Asta, O. Warschkow, D. E. Ellis, L. D. Marks, *Nature* **2002**, *419*, 55-58.

[12] E. Heifets, S. Piskunov, E. A. Kotomin, Y. F. Zhukovskii, D. E. Ellis, *Phys. Rev. B* **2007**, *75*, 115417.

[13] Z. Wang, A. Loon, A. Subramanian, S. Gerhold, E. McDermott, J. A. Enterkin, M. Hieckel, B. C. Russell, R. J. Green, A. Moewes, J. Guo, P. Blaha, M. R. Castell, U. Diebold, L. D. Marks, *Nano Letters* **2016**, *16*, 2407-2412.

[14] a) Y. Peng, W. Si, J. Luo, W. Su, H. Chang, J. Li, J. Hao, J. Crittenden, *Environ. Sci. Technol.* **2016**, *50*, 6442-6448; b) L. C. Seitz, C. F. Dickens, K. Nishio, Y. Hikita, J. Montoya, A. Doyle, C. Kirk, A. Vojvodic, H. Y. Hwang, J. K. Norskov, T. F. Jaramillo, *Science* **2016**, *353*, 1011-1014.

[15] Y. Lin, J. Wen, L. Hu, R. M. Kennedy, P. C. Stair, K. R. Poeppelmeier, L. D. Marks, *Physical Review Letters* **2013**, *111*, 156101.

[16] a) Z. M. Wang, X. F. Hao, S. Gerhold, Z. Novotny, C. Franchini, E. McDermott, K. Schulte, M. Schmid, U. Diebold, *Journal of Physical Chemistry C* **2013**, *117*, 26060-26069; b) R. A. Evarestov, A. V. Bandura, V. E. Alexandrov, *Surface Science* **2007**, *601*, 1844-1856; c) H. J. Zhang, G. Chen, Z. H. Li, *Applied Surface Science* **2007**, *253*, 8345-8351; d) J. A. Rodriguez, S. Azad, L. Q. Wang, J. Garcia, A. Etxeberria, L. Gonzalez, *Journal of Chemical Physics* **2003**, *118*, 6562-6571; e) S. Azad, M. H. Engelhard, L.-Q. Wang, *The Journal of Physical Chemistry B* **2005**, *109*, 10327-10331; f) J. M. P. Martirez, S. Kim, E. H. Morales, B. T. Diroll, M. Cargnello, T. R. Gordon, C. B. Murray, D. A. Bonnell, A. M. Rappe, *Journal of the American Chemical Society* **2015**, *137*, 2939-2947; g) B. Stöger, M. Hieckel, F. Mittendorfer, Z. Wang, D. Fobes, J. Peng, Z. Mao, M. Schmid, J. Redinger, U. Diebold, *Physical Review Letters* **2014**, *113*, 116101; h) R. Hammami, H. Batis, C. Minot, *Surface Science* **2009**, *603*, 3057-3067; i) K. A. Stoerzinger, R. Comes, S. R. Spurgeon, S. Thevuthasan, K. Ihm, E. J. Crumlin, S. A. Chambers, *Journal of Physical Chemistry Letters* **2017**, *8*, 1038-1043; j) A. V. Bandura, R. A. Evarestov, D. D. Kuruch, *Surface Science* **2010**, *604*, 1591-1597; k) R. A. Evarestov, A. V. Bandura, E. N. Blokhin, *Journal of Physics: Conference Series* **2007**, *93*, 1-10; l) K. A. Stoerzinger, W. T. Hong, E. J. Crumlin, H. Bluhm, M. D. Biegalski, Y. Shao-Horn, *Journal of Physical Chemistry C* **2014**, *118*, 19733-19741; m) H. Kizaki, K. Kusakabe, *Surface Science* **2012**, *606*, 337-343; n) I. W. Boateng, R. Tia, E. Adei, N. Y. Dzade, C. R. A. Catlow, N. H. De Leeuw, *Physical Chemistry Chemical Physics* **2017**, *19*, 7399-7409; o) G. Pilania, R. Ramprasad, *Surface Science* **2010**, *604*, 1889-1893.

[17] G. Tesquet, J. Faye, F. Hosoglu, A.-S. Mamede, F. Dumeignil, M. Capron, *Applied Catalysis A: General* **2016**, *511*, 141-148.

[18] a) H. R. J. ter Veen, T. Kim, I. E. Wachs, H. H. Brongersma, *Catal. Today* **2009**, *140*, 197-201; b) S. P. Phivilay, A. A. Puretzky, K. Domen, I. E. Wachs, *ACS Catal.* **2013**, *3*, 2920-2929.

[19] R. Bachelet, F. Sánchez, F. J. Palomares, C. Ocal, J. Fontcuberta, *Applied Physics Letters* **2009**, *95*, 141915.

[20] J. Liu, D. Olds, R. Pend, L. Yu, G. S. Foo, S. Qian, J. Keum, B. Gui-ton, Z. Wu, K. Page, *Chem. Mater.* **2017**.

[21] G. S. Foo, F. Polo-Garzon, V. Fung, D.-e. Jiang, S. H. Overbury, Z. Wu, *ACS Catal.* **2017**, *7*, 4423-4434.

10.1002/anie.201704656

WILEY-VCH

Table of Contents

COMMUNICATION

Controlling the surface termination of $SrTiO_3$, via thermal pretreatment (Sr-enrichment) and chemical etching (Ti-enrichment), showed great potential in tuning catalytic selectivities in a wide range using the conversion of 2-propanol as a probe reaction.

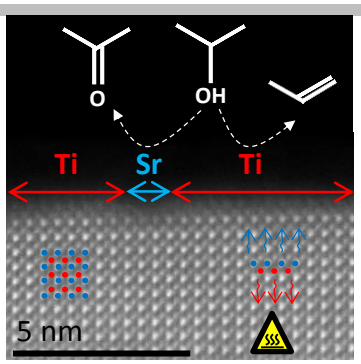

*Felipe Polo-Garzon, Shi-Ze Yang, Victor Fung, Guo Shiou Foo, Elizabeth E. Bickel , Matthew F. Chisholm, De-en Jiang, Zili Wu**

Controlling Reaction Selectivity via Surface Termination of Perovskite Catalysts